

The Integer Quantum Hall Effect

Course Project for PHY 538: Special Topics in Condensed Matter

Wahaj Ayub

23100023

LUMS, School of Sciences and Engineering

May 24, 2022

Abstract

Contents

1	Introduction	2
2	Landau Quantization	2
2.1	Landau Gauge	4
2.1.1	Degeneracy	6
2.2	Background Electric Field	6
3	Berry's Phase and Spectral Flow	8
3.1	Spectral Flow and Aharonov-Bohm Effect	9
3.2	Mathematical Details	10
4	Conductivity in Classical and Quantum Mechanics	12
4.1	Classical Treatment	12
4.2	Semi-Classical Treatment	13
4.3	Conductivity for a Single Particle	13
4.4	Full Quantum Mechanical Treatment Using Linear Response Theory	14
5	The Integer Quantum Hall Effect	14
5.1	Edge States	15
5.2	The Role of Disorder	17
5.3	The Role of Gauge Invariance	19
6	The Role of Topology	19
7	Conclusion	22

1 Introduction

The quantum Hall effect was first discovered by Klaus von Klitzing in 1980 [1]. The discovery marked a new horizon in condensed matter physics and is one of the first well studied so-called topological phenomena in condensed matter. The quantization of the Hall effect is

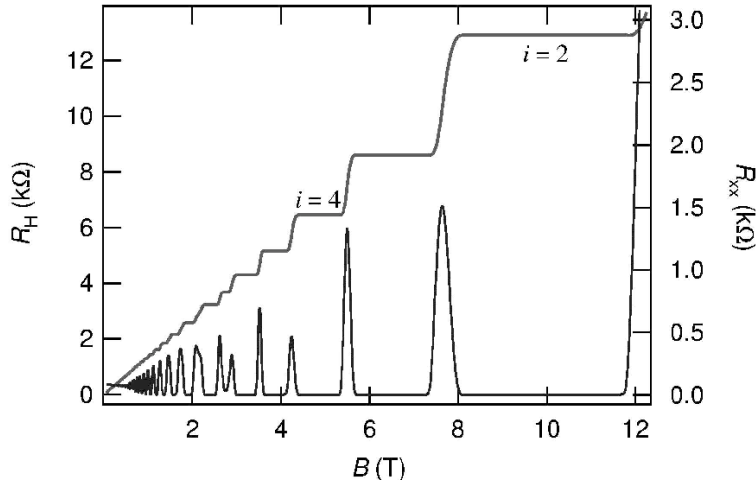


Figure 1: Experimental measurements of the Hall resistance R_H and of the longitudinal resistance R_{xx} for a GaAs/AlGaAs heterostructure at a temperature of 0.1 K [2]

remarkable, as it showed many seemingly peculiar features that had not been observed before. Not only was the Hall conductance quantized in terms of integer multiples of $\frac{e^2}{h}$, it attained these values in the presence of disorder and over a range of magnetic field values. These plateaux and the sharp transitions between them puzzled physicists, before seminal papers by Laughlin [3] and Thouless et. al. [4] shed some light on the matter. Ultimately, this ended with the discovery of deep connection between physics and topology.

Over the years, many similar phenomena such as the fractional quantum Hall effect, which was discovered by Tsui and Stormer in 1982 [5], as well as the anomalous quantum Hall effect in graphene [6] were observed. While the exact details have varied, they have included a consistent theme of topological robustness of these states that allows them to be found in nature without fine-tuning values and allows them to have unique properties.

In this report, we will attempt to describe the mechanism behind the integer quantum Hall effect in terms of conductivity, edge states, disorder, gauge invariance and ofcourse, topology.

2 Landau Quantization

Before we move on to the actual treatment of the quantum Hall effect, we need to consider quantum mechanically, the background in which it can take place. For this, we need to consider a two-dimensional electron gas, freely moving, under the influence of a magnetic field. This results in the phenomenon of Landau levels. The addition of even a small magnetic field drastically changes the energy landscape of the electron gas, as the energies

become quantized. The Hamiltonian for a charged particle with charge $-e$ and mass m is given by [7]

$$H = \frac{1}{2m}(\mathbf{p} + e\mathbf{A})^2. \quad (2.1)$$

Now we can attempt to derive the energy spectrum of the Hamiltonian. Note that since we are working with a 2D gas, our vectors will also be written with two components. We will take our magnetic field to be perpendicular to this plane, or in other words $\mathbf{B} = \nabla \times \mathbf{A} = B\hat{\mathbf{z}}$.

We can define a new operator called the mechanical momentum $\boldsymbol{\pi}$:

$$\boldsymbol{\pi} := \mathbf{p} + e\mathbf{A} \quad (2.2)$$

Using this ‘mechanical momentum’ our Hamiltonian looks just like that of the free particle

$$H = \frac{\boldsymbol{\pi}^2}{2m}. \quad (2.3)$$

However, the mechanical momentum is not canonical: it does not satisfy the required commutation relations. This can be shown either using Poisson brackets from classical mechanics, or by imposing the canonical commutation relations of quantum mechanics on \mathbf{p} [7]. This is taken to be the canonical momentum as it derived using the derivatives of the Lagrangian with respect to $\dot{\mathbf{x}}$. The resulting commutation relations for $\boldsymbol{\pi}$ are

$$[\pi_x, \pi_y] = -ie\hbar B. \quad (2.4)$$

Now, we can introduce raising and lowering operators that show us how we can solve the problem, just as if it were a harmonic oscillator.

$$a = \frac{1}{\sqrt{2e\hbar B}}(\pi_x - i\pi_y) \quad a^\dagger = \frac{1}{\sqrt{2e\hbar B}}(\pi_x + i\pi_y)$$

We can work out the commutation relations for these operators:

$$\begin{aligned} [a, a^\dagger] &= \frac{1}{2e\hbar B}[\pi_x - i\pi_y, \pi_x + i\pi_y], \\ &= \frac{1}{2e\hbar B}(i[\pi_x, \pi_y] - i[\pi_y, \pi_x]), \\ &= \frac{1}{2e\hbar B}2i[\pi_x, \pi_y], \\ &= \frac{1}{2e\hbar B}2e\hbar B, \\ &= 1. \end{aligned}$$

Using this, we can easily show that the Hamiltonian can be written exactly like the harmonic oscillator [7]

$$H = \hbar\omega_B \left(a^\dagger a + \frac{1}{2} \right),$$

where $\omega_B = \frac{eB}{m}$ is called the cyclotron frequency. Using, the exact arguments as for a harmonic oscillator [8], we can then argue that the energies are quantized and the eigenvalues are given by

$$E_n = \hbar\omega_B \left(n + \frac{1}{2} \right) \quad n \in \mathbb{N} \quad (2.5)$$

These energy levels are called the Landau levels. However, notice that our original system was a two dimensional system and the energies here look exactly like a one dimensional harmonic oscillator. This is because there is a hidden degeneracy in the energy levels that is not shown here. To explore that, we will make a specific gauge choice for the potential \mathbf{A} and then find the wavefunctions for each state. One convenient choice for such a gauge is the Landau gauge.

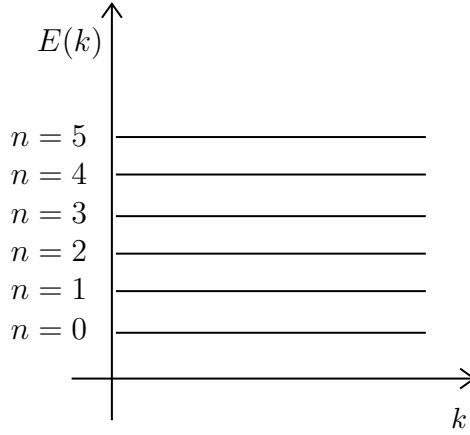


Figure 2: Landau Levels

2.1 Landau Gauge

The most common gauge choice when dealing with the integer quantum Hall effect is the **Landau gauge** [9],

$$\mathbf{A} = xB\hat{y}. \quad (2.6)$$

Notice that although the physics of the system should be invariant under translation along both the x and y axis, this is not true for the specific gauge we have chosen. This means that the Hamiltonian, in intermediate stages, will look as if it has no translational symmetry in the x -axis. Expanding everything out, the Hamiltonian in the Landau gauge becomes

$$H = \frac{1}{2m} (p_x^2 + (p_y + eBx)^2).$$

Due to translational symmetry in the y -direction, an ansatz of the following form is useful [7]

$$\psi_k(x, y) = e^{iky} f_k(x). \quad (2.7)$$

This is an eigenstate of p_y , that can be replaced by the eigenvalue $\hbar k$ when acting the Hamiltonian on this wavefunction. The effective 1D Schrodinger equation then becomes

$$H\psi_k(x, y) = \frac{1}{2m} (p_x^2 + (\hbar k + eBx)^2) \psi_k(x, y) := H_k\psi_k(x, y).$$

We define a new quantity called the magnetic length $l_B := \sqrt{\frac{\hbar}{eB}}$, and perform algebraic manipulations to bring out the form of a displaced 1D oscillator with frequency ω_B

$$H_k = \frac{1}{2m}p_x^2 + \frac{m\omega_B^2}{2}(x + kl_B^2)^2. \quad (2.8)$$

For any given value of k there will be a family of energy eigenstates with eigenvalues

$$E_{k,n} = \hbar\omega_B \left(n + \frac{1}{2} \right),$$

which depend on the Landau level n , but not on the y -momentum. The corresponding eigenstates can then be given in terms of Hermite polynomials H_n :

$$\psi_{n,k}(x, y) = e^{iky} H_n(x + kl_B^2) e^{-(x+kl_B^2)^2/2l_B^2}, \quad (2.9)$$

where these functions have not been normalized. It is important to note that these wavefunctions are gauge dependent quantities, and on there own there exact shape can vary wildly depending on the gauge choice [7]. For example, in the Landau gauge, the wavefunctions are strip like, while for another popular choice, the symmetric gauge, they form concentric circles around some origin point.

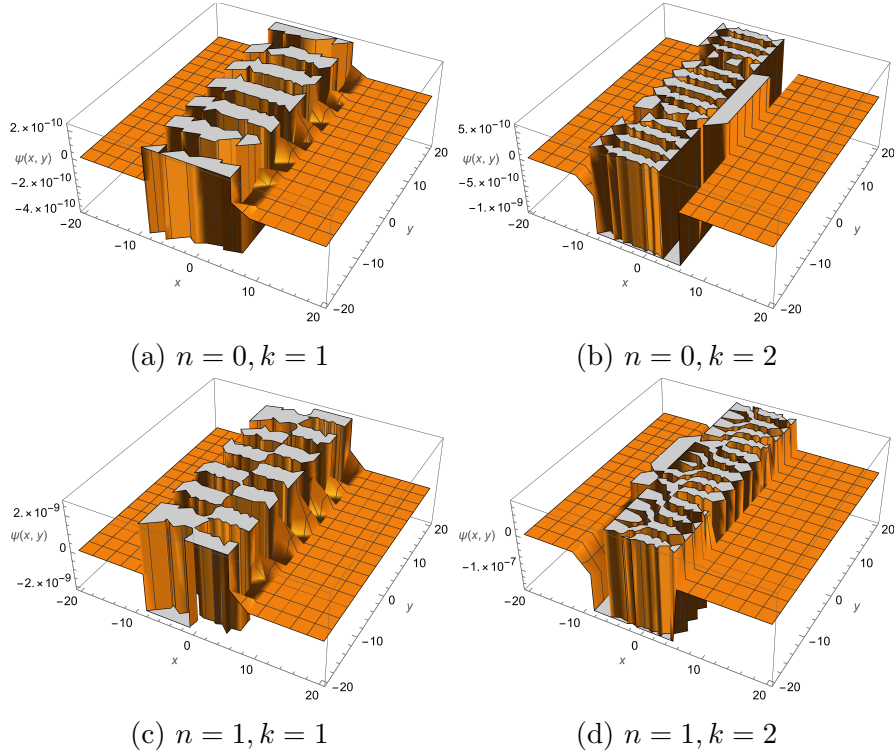


Figure 3: Plots of the ‘strip-like’ wavefunctions in the Landau gauge. The axes are in units of l_B

We can calculate the group velocity of the electrons in the y direction using [9]

$$v_y = \frac{1}{\hbar} \frac{\partial E_{n,k}}{\partial k} = 0. \quad (2.10)$$

It is prudent to notice that we've been treating the particles as if they are allowed to move freely in 2D plane. This is a valid approximation as long as the magnetic length l_B^2 is much greater than the lattice constant, that is, as long as the effective mass approximation is valid [9]. Using the effective mass m^* instead of the mass of the electron would provide a better approximation.

2.1.1 Degeneracy

In order to count the degeneracy in the Landau levels, we need to count the number of states in each one. The following argument adapted from both Refs. [7] and [9] is somewhat heuristic, but gives the correct number of degenerate states. We want to restrict our system to a finite size of $L_x \times L_y$. We assume periodic boundary conditions in the y direction. For the x -direction, we cannot do this so we must rely on the fact that away from the center of each wavefunction $x = -kl_B^2$, the wavefunctions rapidly decay. If we restrict our sample to $0 \leq x \leq L_x$, we expect that the allowed k values would range $-L_x/l_B^2 \leq k \leq 0$ [7]. Then, we can simply count states

$$N = \frac{L_y}{2\pi} \int_{-L_x/l_B^2}^0 dk = \frac{L_x L_y}{2\pi l_B^2} = \frac{eBA}{2\pi\hbar}. \quad (2.11)$$

We define the quantum of flux Φ_0 as

$$\Phi_0 := \frac{2\pi\hbar}{e}, \quad (2.12)$$

allowing us to write $N = \frac{AB}{\Phi_0}$. This is a very large degeneracy and plays an important role in phenomena of quantum Hall effects.

2.2 Background Electric Field

We can modify this system by adding an electric field. This modifies the Hamiltonian by adding an electric potential $\phi = -Ex$. The Hamiltonian then becomes

$$H' = \frac{1}{2m} (p_x^2 + (p_y + eBx)^2) + eEx. \quad (2.13)$$

We can complete the square here, by first expanding everything out. Note that since there is still translational invariance in the y -direction, our ansatz should still work, and we will

build on from the Hamiltonian in Eq. 2.8:

$$\begin{aligned}
H'_k &= \frac{1}{2m} p_x^2 + \frac{m\omega_B^2}{2} (x + kl_B^2)^2 + eEx \\
&= \frac{1}{2m} p_x^2 + \frac{m\omega_B^2}{2} (x^2 + k^2 l_B^4 + 2kl_B^2 x) + eEx \\
&= \frac{1}{2m} p_x^2 + \frac{m\omega_B^2}{2} \left(x^2 + 2 \left(kl_B^2 + \frac{eE}{m\omega_B^2} \right) x + k^2 l_B^4 \right) \\
&= \frac{1}{2m} p_x^2 + \frac{m\omega_B^2}{2} \left(x^2 + 2 \left(kl_B^2 + \frac{eE}{m\omega_B^2} \right) x + \left(kl_B^2 + \frac{eE}{m\omega_B^2} \right)^2 - \left(kl_B^2 + \frac{eE}{m\omega_B^2} \right)^2 + k^2 l_B^4 \right) \\
&= \frac{1}{2m} p_x^2 + \frac{m\omega_B^2}{2} \left(x + kl_B^2 + \frac{eE}{m\omega_B^2} \right)^2 + \frac{m\omega_B^2}{2} \left(k^2 l_B^4 - \left(kl_B^2 + \frac{eE}{m\omega_B^2} \right)^2 \right) \\
&= \frac{1}{2m} p_x^2 + \frac{m\omega_B^2}{2} \left(x + kl_B^2 + \frac{eE}{m\omega_B^2} \right)^2 + \frac{m\omega_B^2}{2} \left(-\frac{e^2 E^2}{m^2 \omega_B^4} - 2 \frac{eE kl_B^2}{m\omega_B^2} \right) \\
&= \frac{1}{2m} p_x^2 + \frac{m\omega_B^2}{2} \left(x + kl_B^2 + \frac{mE}{eB^2} \right)^2 - eE \left(kl_B^2 + \frac{eE}{m\omega_B^2} \right) + \frac{m}{2} \frac{E^2}{B^2}.
\end{aligned}$$

In the last step, we have used the definition of ω_B^2 to simplify some parts. The energies are then easily read off, as it just involves a harmonic oscillator plus some constant term (which depends linearly on k):

$$E'_{n,k} = \hbar\omega_B \left(n + \frac{1}{2} \right) - eE \left(kl_B^2 + \frac{eE}{m\omega_B^2} \right) + \frac{m}{2} \frac{E^2}{B^2}. \quad (2.14)$$

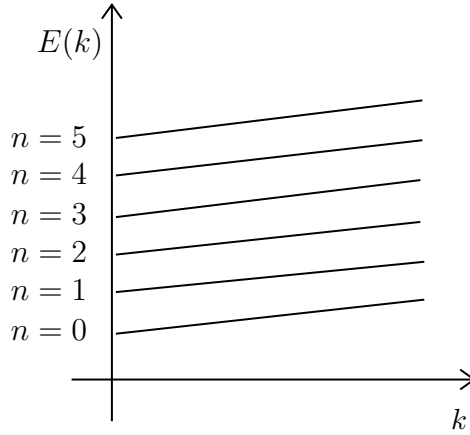


Figure 4: The degeneracy has been removed

Clearly, the energies now depend on the momentum and the group velocity is [7]

$$v'_y = \frac{1}{\hbar} \frac{\partial E_{n,k}}{\partial k} = -\frac{e}{\hbar} l_B^2 = -\frac{E}{B}.$$

So the final term in $E'_{n,k}$ can be thought as the kinetic energy $\frac{1}{2}mv_y^2$ due to movement in the y direction.

3 Berry's Phase and Spectral Flow

An essential key to understanding the topological aspects of the integer quantum Hall effect is the concept of Berry's phase. This was introduced in 1984 by Micheal Berry, and is an additional phase factor that arises from slowly varying a vector of parameters $\boldsymbol{\lambda}$ that controls the Hamiltonian, and ultimately bringing them back to the same place. According to the adiabatic theorem, if we vary the parameters slowly enough, we should 'stick' to the energy eigenstate and if we end up back at the same parameters, we should end up in the same state, perhaps with the addition of the some phase factor [10]. In other words, if we trace out a closed path in the space of parameters, our state should evolve as [7]

$$|\psi\rangle \rightarrow e^{i\gamma} |\psi\rangle. \quad (3.1)$$

We know that any quantum mechanical state evolves using the time-dependent Schrodinger equation

$$i\hbar \frac{\partial |\psi\rangle}{\partial t} = H[\boldsymbol{\lambda}(t)] |\psi\rangle. \quad (3.2)$$

Now we use the adiabatic ansatz, which says that if we start out in the n^{th} state

$$|\psi(t=0)\rangle = |n[\boldsymbol{\lambda}(t=0)]\rangle, \quad (3.3)$$

then it will evolve into the n^{th} eigenstate at later times as well [9]

$$|\psi(t)\rangle = C(t) |n[\boldsymbol{\lambda}(t)]\rangle. \quad (3.4)$$

Here $C(t)$ is some time dependent phase factor, since the time evolution under H must be unitary. Additionally, we can factor out the 'dynamical part' of the phase factor C :

$$C(t) = e^{i\gamma(t)} e^{-\frac{i}{\hbar} \int_0^t E_n(t') dt'}. \quad (3.5)$$

We will ignore the dynamical part, as it is not what we are interested in. Putting Eq. 3.4 into Eq. 3.2, and then taking an inner product with $\psi(t)$, we get:

$$\frac{\partial \gamma}{\partial t} = i \langle n[\boldsymbol{\lambda}(t)] | \frac{\partial}{\partial t} | n[\boldsymbol{\lambda}(t)] \rangle, \quad (3.6)$$

$$\frac{\partial \gamma}{\partial t} = i \langle n[\boldsymbol{\lambda}(t)] | \nabla_{\boldsymbol{\lambda}} | n[\boldsymbol{\lambda}(t)] \rangle \cdot \frac{d\boldsymbol{\lambda}}{dt}, \quad (3.7)$$

$$\frac{\partial \gamma}{\partial t} = i \langle n[\boldsymbol{\lambda}(t)] | \frac{\partial}{\partial \lambda^i} | n[\boldsymbol{\lambda}(t)] \rangle \cdot \dot{\lambda}^i, \quad (3.8)$$

$$(3.9)$$

where in the last line, we have used Einstein summation convention. This easily leads to the solution for $\gamma(t)$ as

$$\gamma(t) = i \int_{\boldsymbol{\lambda}(0)}^{\boldsymbol{\lambda}(t)} \langle n[\boldsymbol{\lambda}(t)] | \nabla_{\boldsymbol{\lambda}} | n[\boldsymbol{\lambda}(t)] \rangle \cdot d\boldsymbol{\lambda}. \quad (3.10)$$

This is a convenient time to define the Berry connection

$$\mathcal{A}(\boldsymbol{\lambda}) = i \langle n[\boldsymbol{\lambda}] | \nabla_{\boldsymbol{\lambda}} | n[\boldsymbol{\lambda}] \rangle, \quad (3.11)$$

which can be written in coordinates as

$$\mathcal{A}_i(\boldsymbol{\lambda}) = i \langle n[\boldsymbol{\lambda}] | \frac{\partial}{\partial \lambda^i} | n[\boldsymbol{\lambda}] \rangle . \quad (3.12)$$

Now, the phase factor can be simply written as

$$\gamma(t) = \int_{\boldsymbol{\lambda}(0)}^{\boldsymbol{\lambda}(t)} \boldsymbol{\mathcal{A}} \cdot d\boldsymbol{\lambda} . \quad (3.13)$$

If we consider a closed path, that ends at the same point it started at, we finally have Berry's phase:

$$e^{i\gamma} = \exp \left(\oint \boldsymbol{\mathcal{A}} \cdot d\boldsymbol{\lambda} \right) . \quad (3.14)$$

One important fact about the Berry's phase is that it is gauge independent. Another gauge independent quantity that we can consider is the 'curvature' of the connection, which is a gauge invariant field strength:

$$\mathcal{F}_{ij}(\boldsymbol{\lambda}) = \frac{\partial \mathcal{A}_j}{\partial \lambda^i} - \frac{\partial \mathcal{A}_i}{\partial \lambda^j} . \quad (3.15)$$

Berry's phase can also be written in terms of the 'flux' of the field strength [7]:

$$e^{i\gamma} = \exp \left(\oint \mathcal{A}_i d\lambda^i \right) = \exp \left(\int_S \mathcal{F}_{ij} dS^{ij} \right) . \quad (3.16)$$

3.1 Spectral Flow and Aharonov-Bohm Effect

One interesting physical side-effect of Berry's phase is that classically 'unphysical' quantities such as the gauge potential of the electromagnetic field can in certain circumstances cause physical consequences. Consider particles moving around a flux tube, with a fixed magnetic flux Φ through it, but no magnetic field in the region in which the particle moves. The gauge potential \mathbf{A} can be solved for in polar coordinates as

$$A_\phi = \frac{\Phi}{2\pi r} , \quad (3.17)$$

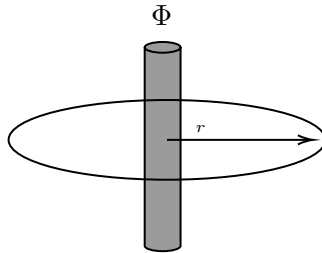


Figure 5: Particle around a flux tube

with all other components vanishing. If we restrict our particle to only move at a fixed radius, we have an effective 1D problem with the Hamiltonian [7]

$$H = \frac{1}{2m}(p_\phi + A_\phi)^2 = \frac{1}{2mr^2}(-i\hbar\frac{\partial}{\partial\phi} + \frac{e\Phi}{2\pi})^2. \quad (3.18)$$

We guess the wavefunctions

$$\psi = \frac{1}{\sqrt{2\pi r}}e^{-in\phi}, \quad (3.19)$$

where the ns need to be integers for the function to be single valued. This gives us the energy spectrum [7]

$$E = \frac{\hbar^2}{2mr^2} \left(n - \frac{\Phi}{\Phi_0} \right)^2. \quad (3.20)$$

Now, notice that if we increase the flux Φ , gradually from 0 to Φ_0 , the n^{th} energy eigenstate is shifted to the next level $n + 1$. This is called spectral flow, and will form an essential part of our discussion on how gauge invariance plays a role in the quantized Hall effect.

The setup described above can be altered slightly to consider something called the Aharonov-Bohm effect. We will not describe the details of this effect and it can be found in many standard books about quantum mechanics such as Ref. [10]. However, the short version is that, the gauge potential can cause a phase factor that depends on the path taken. If we perform a typical double split experiment between two electrons, with a solenoid with flux Φ in between, the interference pattern is change, unless the flux is an integer multiple of Φ_0 .

3.2 Mathematical Details

The deep geometric meaning behind Berry's phase can be understood in the language of differential geometry, where Berry's phase can be described as a holonomy in the parameter space [11]. To describe what this means exactly, we need to understand what a fibre bundle is, and how it is related to connections and curvature. This will also explain why we previously named the Berry connection and curvature using those terms. In order to keep it brief, these ideas will only be described to a certain degree.

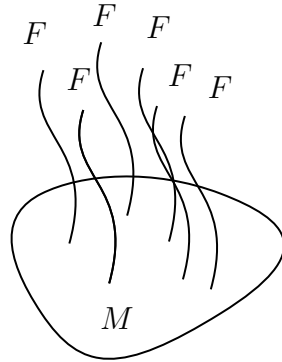


Figure 6: A pictorial representation of a fibre bundle

A **smooth manifold** M is a space that locally looks like Euclidean space, and can given some differential structure [11]. A **fibre bundle** with typical fibre F can be thought of as a triplet (E, F, M) , such that E , called the total space, can be written locally as a product $M \times F$ [12]. Additionally, a projection operator $\pi : E \rightarrow M$ needs to be defined, which takes points in the fibre bundle to the point in the manifold where the fibre is attached. This can be thought of as attaching a fibre F at every point of M . We can also have some structure group G that can act on the fibre to take us from one point to the other. If the fibre F is isomorphic (or it looks like) G , then we have something called a **principle fibre bundle** [12]. A **connection** on the bundle is some way to ‘transport’ elements from one fibre to elements of the neighbouring fibres in a smooth manner. The **curvature** associated to the connection is 2-form (or an anti-symmetric (02) tensor) that tells us the degree to which the connection is ‘curved’ [11].

If we have a closed path $\gamma : [0, 1] \rightarrow M$ in a manifold M that ends and begins at $x_0 \in M$, we can **lift** it to a path $\tilde{\gamma} : [0, 1] \rightarrow E$ in the principle bundle E . However, this path need not be closed. The only requirement is that $\tilde{\gamma}(0)$ and $\tilde{\gamma}(1)$ both need to lie in the same fibre. Since, in this case, the fibre is a group G , the elements can be related to each other via some group element. This group element is said to be part of the **holonomy group** [11]. A **holonomy** in some sense measures how different these elements are.

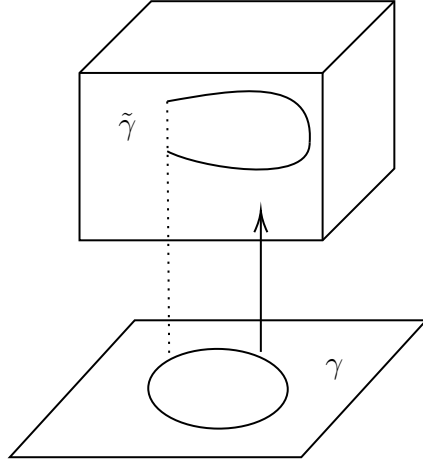


Figure 7: Pictorial representation of a horizontal lift

Now, in the context of Berry’s phase, we consider our parameter space as the manifold, which is described by local coordinates $\boldsymbol{\lambda}$. We consider each point to correspond to the n^{th} eigenstate $|n[\boldsymbol{\lambda}]\rangle$. However, since I could also choose $e^{i\phi} |n[\boldsymbol{\lambda}]\rangle$. So, we need to consider the a $U(1)$ degree of freedom each point [11], and hence we have a $U(1)$ principal bundle E , where a typical element can be represented as $e^{i\phi} |n[\boldsymbol{\lambda}]\rangle$. The projection operator gives us $\pi(e^{i\phi} |n[\boldsymbol{\lambda}]\rangle) = \boldsymbol{\lambda}$. Now, we can check that the Berry’s connection provided above is a connection on the manifold and \mathcal{F}_{xy} is the associated curvature form. Now, if see what we were doing before, we traced out a closed loop in the parameter space, and then ‘lifted’ it to the fibre bundle by considering the resulting quantum state. Now, we finally, consider how the fibres, the quantum states, are different before and after completing the loop, in terms

of a group element $g \in U(1)$, that we call Berry's phase. So, Berry's phase is a holonomy in the parameter space.

4 Conductivity in Classical and Quantum Mechanics

In this section we will see how we can deal with various treatments of conductivity, and specifically Hall conductivity that can provide a basis for understanding the integer quantum Hall effect in a rigorous manner.

4.1 Classical Treatment

In classical electricity and magnetism, the conductivity of a material is defined to be constant such that $\mathbf{J} = \sigma \mathbf{E}$. However, when considering the action of both a magnetic and electric field together, we see that there can be currents that are perpendicular to both. Hence the conductivity (and resistivity ρ) become tensors [9]

$$J_i = \sigma_{ij} E_j, \quad (4.1)$$

$$E_i = \rho_{ij} J_j, \quad (4.2)$$

where Einstein summation convention has been used. Now, we can analyse the transport of electrons under a magnetic field using the **Drude model** [13].

The Drude model involves a particle placed in side a magnetic field \mathbf{B} , an electric field \mathbf{E} that can accelerate the charges and a linear friction term that represents the effects of 'collisions'. This gives us the following equation of motion [13]

$$\frac{d\mathbf{p}}{dt} = -e(\mathbf{E} + \mathbf{v} \times \mathbf{B}) - \mathbf{p}/\tau, \quad (4.3)$$

where τ is called the scattering time. We are interested in equilibrium solutions, so we set $\frac{d\mathbf{p}}{dt} = 0$. Using $\mathbf{p} = m\mathbf{v}$ and $\mathbf{J} = -nev$, we get

$$0 = -e\mathbf{E} + \frac{\mathbf{J} \times \mathbf{B}}{n} + \frac{m}{ne\tau}\mathbf{J}. \quad (4.4)$$

Now, we suppose that the magnetic field $\mathbf{B} = B\hat{\mathbf{z}}$. Since, we are only interested in the 2D plane, we will restrict our attention to those components. The resistivity tensor can be written as

$$\mathbf{E} = \rho \mathbf{J},$$

where

$$\rho = \frac{m}{ne^2\tau} \begin{bmatrix} 1 & \frac{eB\tau}{m} \\ -\frac{eB\tau}{m} & 1 \end{bmatrix}. \quad (4.5)$$

Now, in this specific case the Hall resistance (which we can actually measure) coincides with the Hall conductivity. The transverse resistance can be calculated as

$$R_{xy} = -\rho_{xy}.$$

Additionally, for any current I_x in the x -direction, and an associated electric field E_y in the y -direction we can define the Hall coefficient R_H as

$$R_H = -\frac{E_y}{J_x B} = \frac{\rho_{xy}}{B},$$

which for the Drude model, would become $R_H = \frac{1}{ne}$.

Now, we have all we need classically to predict both the resistivities ρ_{xx} and ρ_{xy} , which we can then measure.

4.2 Semi-Classical Treatment

We can give a heuristic semi-classical argument for why the Hall conductivity when ν Landau levels are filled should be equal to the value given by the integer quantum Hall effect. Now, from the Drude model, we have an expression for ρ_{xy} . If exactly ν Landau levels are filled the corresponding electron density will be given by

$$n = \frac{N}{A} = \frac{B}{\Phi_0} \nu, \quad (4.6)$$

giving us

$$\rho_{xy} = \frac{B\Phi_0}{eB\nu} = \frac{2\pi\hbar}{e^2} \frac{1}{\nu}.$$

Additionally, when ν Landau levels are filled, there is an energy gap, and no low lying excitations, so we have an insulator and hence $\tau \rightarrow \infty$ and consequently $\rho_{xx} \rightarrow 0$. However, this only works for when there is exact filling. It does not explain the existence of a plateau.

4.3 Conductivity for a Single Particle

We can also describe conductivity for a single free particle using quantum mechanics [7]. If the velocity of a particle is given by $\dot{\mathbf{x}} = \frac{\mathbf{p} + e\mathbf{A}}{m}$, then current operator will be given by

$$\hat{\mathbf{I}} = -e \frac{\mathbf{p} + e\mathbf{A}}{m}.$$

The expectation value for the current will be given by [7]

$$\mathbf{I} = -\frac{e}{m} \sum_{\text{filled states}} \langle \psi | -i\hbar\nabla + e\mathbf{A} | \psi \rangle. \quad (4.7)$$

When ν Landau levels are filled,

$$I_x = 0,$$

and

$$\begin{aligned}
I_y &= -\frac{e}{m} \sum_{n=1}^{\nu} \sum_k \langle \psi_{n,k} | -i\hbar \frac{\partial}{\partial y} + eBx | \psi_{n,k} \rangle, \\
&= -\frac{e}{m} \sum_{n=1}^{\nu} \sum_k \langle \psi_{n,k} | \hbar k + eBx | \psi_{n,k} \rangle, \\
&= -\frac{e}{m} \sum_{n=1}^{\nu} \sum_k \hbar k + \langle \psi_{n,k} | eBx | \psi_{n,k} \rangle, \\
&= -\frac{e}{m} \sum_{n=1}^{\nu} \sum_k \frac{-mE}{B}, \\
&= e \sum_{n=1}^{\nu} \sum_k \frac{E}{B}, \\
&= eE\nu \frac{A}{\Phi_0}.
\end{aligned}$$

This gives us $\mathbf{J} = \begin{pmatrix} 0 \\ eE\nu\Phi_0 \end{pmatrix}$, which corresponds exactly with the resistivities at the plateaux.

4.4 Full Quantum Mechanical Treatment Using Linear Response Theory

While a single particle treatment can suffice for some purposes, we will need to consider a many body treatment of the problem if we are to consider, for example, topological effects. This can be done through linear response theory and something called the Kubo formula. The derivation involves the use of time dependent perturbation theory to derive the following result for a system that starts out in the state $|0\rangle$:

$$\sigma_{xy} = iA\hbar \sum_{n=0} \frac{\langle 0 | J_y | n \rangle \langle n | J_x | 0 \rangle - \langle 0 | J_x | n \rangle \langle n | J_y | 0 \rangle}{(E_n - E_0)^2}. \quad (4.8)$$

This is called the Kubo formula for Hall conductivity and a detailed derivation can be found in Ref. [7].

5 The Integer Quantum Hall Effect

While we can explain some of the integer quantum Hall effect using a simple analysis of a particle in a magnetic field, the complete picture, including why the plateaux appear over a range of B values, we need to consider the effect of disorder, which causes localization of some states, as well as edge states, which will end up carrying most of the current.

5.1 Edge States

Now we wish to consider a sample for which we have a well-defined boundary for the sample in the x -direction. These can be modelled by a potential $V(x)$, that rises steeply at both ends, and we can take to be constant away from the edge. Since translational symmetry in the y -direction is maintained, we can still see that the wavefunction will be of the form

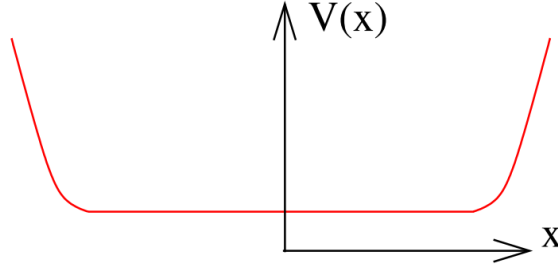


Figure 8: The potential that defines our edges [7]

$$\psi(x, y) = \frac{1}{\sqrt{L_y}} e^{iky} f_k(x). \quad (5.1)$$

Of course, $f_k(x)$ is no longer a simple harmonic wave function, but they would have a similar character, such as being peaked near $X = -kl_B^2$. The group velocity would then be given by, using a Taylor expansion around this position, [7]

$$v_y = -\frac{1}{eB} \frac{\partial V}{\partial x}. \quad (5.2)$$

So, each wavefunction would sit at a different position, with a different velocity. Importantly,

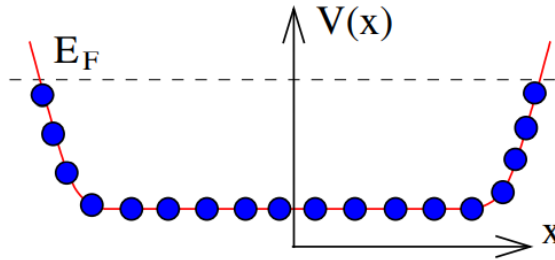


Figure 9: Filled states [7]

at both edges, we have **chiral** modes, which travel in different directions. Chiral modes are special, and they can only exist at the boundary of a system [7]. These chiral modes are part of the reason why the Hall conductance is quantized even in the presence of disorder.

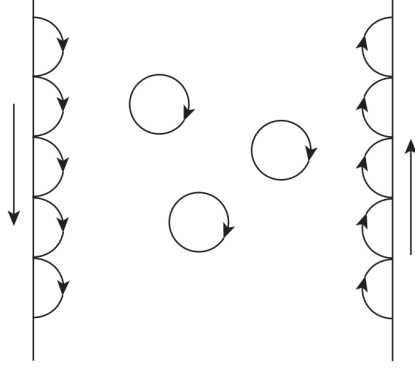


Figure 10: A semi-classical picture which explains the chirality of edge states via lack of back propagation [9]

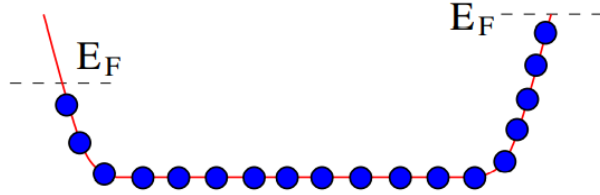


Figure 11: A potential difference is applied across the edges [7]

As k determines the x position (and vice versa), filling our states in according to x value makes sense in this case.

We treat the bulk of the material as an insulator and the edge states as conducting states. We can then simply introduce a potential difference $\Delta\mu$, caused by some Hall voltage V_H . For now, we only assume that a single Landau level is occupied and sum over the occupied states

$$I_y = -e \int \frac{dk}{2\pi} v_y(k) = \frac{e}{2\pi l_B^2} \int dx \frac{1}{eB} \frac{\partial V}{\partial x} = \frac{e}{2\pi\hbar} \Delta\mu. \quad (5.3)$$

Using the fact that $eV_H = \Delta\mu$, we get that

$$\sigma_{xy} = \frac{I_y}{V_H} = \frac{e^2}{2\pi\hbar} \quad (5.4)$$

Now, there is a slight discrepancy, as previously we were assuming that all states contributed to the current equally, but now it seems like we are only counting states that are on the edge. The truth, as always, lies somewhere in the middle. The calculation in Eq. 5.1 works even when there is a random potential $V(x)$ in the middle, as long as it is smooth. So the current is shared among all of the states, however the edge states carry a larger amount of current. We can also think about this in terms of the absence of ‘backscattering’ in the edge states and Landauer model of transport in 1D quantum wires [9].

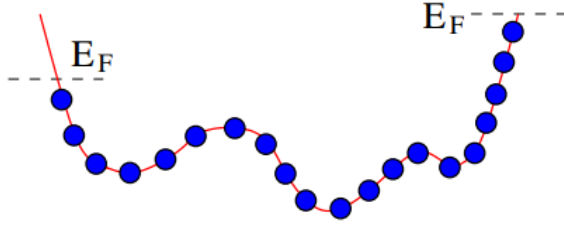


Figure 12: We can also use a random potential [7]

By setting the Fermi energy E_F between two Landau levels, and using a similar argument, we have n filled Landau levels, with n corresponding chiral modes on each edge, giving us

$$\sigma_{xy} = \frac{e^2}{2\pi\hbar} n. \quad (5.5)$$

The calculations above explain why we get the observed longitudinal and Hall conductivities when precisely an integer number of Landau levels are filled, but what about in the middle? Why do the plateaux exist and why is there a sharp transition. These exist due to the presence of the previously mentioned disorder.

5.2 The Role of Disorder

We can model disorder in the system by adding a random potential $V(x)$ to the Hamiltonian. Due to the random potential, which will not have any symmetry, the degeneracies in the Landau levels are broken down. Assuming that we only have weak disorder, which is smaller than the splitting of the Landau levels, this will result in the Landau levels becoming narrow bands. The disorder also turns some of the states in the bulk into localized states, which cannot carry current [9]. This process is called Anderson localization. This is an essential part of why the Hall resistance takes the quantized value over a finite range of magnetic field rather than just at a single point.

For a strong magnetic field, the magnetic length would be small compared to the change in the random potential, and we can use a semi-classical picture to illustrate the effects of disorder. In this limit, we have a semi-classical cyclotron orbit of an electron taking place in a region with roughly constant potential. We define quantum operators X and Y , that define the centre of the orbit [7]

$$X = x - \frac{\pi_y}{m\omega_B} \quad \text{and} \quad Y = y + \frac{\pi_x}{m\omega_B}, \quad (5.6)$$

where $\boldsymbol{\pi}$ is the mechanical momentum. We can also derive the time evolution of these operators, using the Heisenberg equation of motion [7]

$$\begin{aligned} i\hbar\dot{X} &= [X, H + V] = [X, Y] \frac{\partial V}{\partial Y} = il_B^2 \frac{\partial V}{\partial Y}, \\ i\hbar\dot{Y} &= [Y, H + V] = [Y, X] \frac{\partial V}{\partial X} = -il_B^2 \frac{\partial V}{\partial X}. \end{aligned}$$

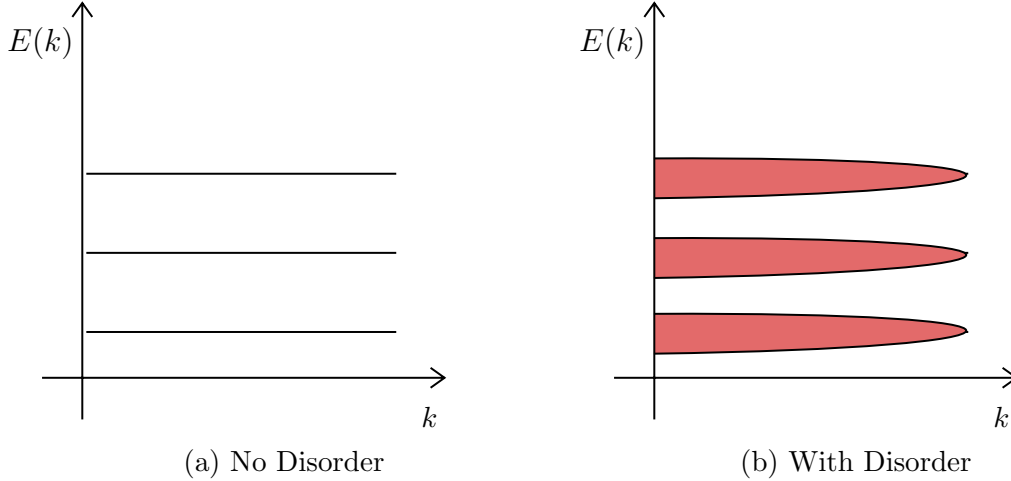


Figure 13: The density of states is broadened due to the presence of disorder

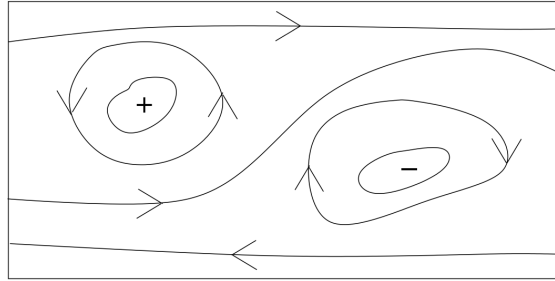


Figure 14: Localization due to the presence of disorder [7]

So, the center of mass drifts perpendicular to ∇V , and hence along equipotentials. Now, for a potential with local maxima and minima, particles will move around these in anti-clockwise and clockwise directions, respectively. However, they cannot move throughout the sample and have become trapped near these extreme points. They are localized and cannot carry current. So the states both at the lower energies and higher energies in the band become localized.

Now, we can look to understand how the plateaux come about. Consider a system where we have filled all of the extended states, but the band has not been fully filled. We will have some left over localized states. Suppose we decrease B while keeping n fixed. This would decrease the number of states in each Landau level. However instead of the next Landau level being filled, the localized states would be filled, without adding to the conductivity. This is why plateaux are observed over a range of B values.

The localization of charges causes there to be less states which can carry current. Does this cause any change in the total current carried? The answer is no, since the edge states correspondingly carry more current. This is due to the role gauge invariance plays in the integer quantum Hall effect.

5.3 The Role of Gauge Invariance

The argument involving how gauge invariance is related to maintaining the quantization of charge, despite the presence of disorder, uses the concept of spectral flow as described in Section 3.1. We consider the ‘Corbino Ring’ geometry, which allows us to add an additional flux that goes through the center of the ring. Suppose we apply an emf \mathcal{E} to the ring by slowly increasing the flux from 0 to Φ_0 , in a time T . The resulting emf would be $\mathcal{E} = \frac{-\Phi_0}{T}$. If n electrons move from the inner ring to the outer ring, the resulting radial current would be $I_r = -ne/T$. This would give us

$$\rho_{xy} = \frac{\mathcal{E}}{I_r} = \frac{2\pi\hbar}{e^2} \frac{1}{n^2}, \quad (5.7)$$

which is of course, the result that we want. Working in the symmetric gauge, wavefunctions are classified by their radial distance [7]. Without the presence of disorder, we can simply consider spectral flow, whereby, an electron in state m would be transferred to state $m + 1$, which would be radially outwards. If all of the states in a Landau level are filled, as we increase to Φ_0 , a single electron is transferred. For n Landau levels, n electrons would be transferred.

Now suppose we also model the presence of disorder, with a random potential $V(r, \phi)$. The Hamiltonian, in polar coordinates and the symmetric gauge $A = -\frac{1}{2}r \times B$, becomes [7]

$$H_\Phi = \frac{1}{2m} \left[-\hbar^2 \frac{1}{r} \frac{\partial}{\partial r} \left(r \frac{\partial}{\partial r} \right) + \left(-\frac{i\hbar}{r} \frac{\partial}{\partial \phi} + \frac{eBr}{2} + \frac{e\Phi}{2\pi r} \right)^2 \right] + V(r, \phi). \quad (5.8)$$

Now, for localized states, we can simply reverse the effects of the flux by a gauge transformation $\psi(r, \phi) \rightarrow e^{-ie\Phi\phi/2\pi\hbar} \psi(r, \phi)$, however, for extended states, we need to make sure that they remain single valued when $\phi \rightarrow \phi + 2\pi$. This implies that this is only possible when $\Phi = n\Phi_0$, for some integer n . So, localized states don’t change when increasing the flux from 0 to Φ_0 but extended states localized at one radius are transferred to the next available extended state. While there may be less extended states, if every extended state in a Landau level is filled, at the end, one electron is passed from the inner ring to the outer part, causing the same result as Eq. 5.7.

6 The Role of Topology

The above results, as well as the fact that the integer quantum Hall effect is resistant to disorder and holds over a finite range of parameters suggest that the effect is topological in nature, relying on the broad features of the system rather than fine tuned parameters. In this part of the report we will look to make this connection between the quantum Hall effect and topology clear, by using the tools we have developed before, including the Kubo formula and Berry’s phase.

We will consider our system now placed on a torus \mathbf{T}^2 , which we can think of as rectangle, whose opposite ends have been glued together. We will take the side lengths to be L_x and L_y .

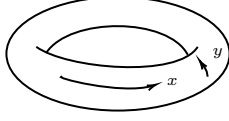


Figure 15: Our torus geometry

Now, we need to consider the boundary conditions of the wavefunction. We cannot directly impose periodic boundary conditions $\psi(x, y) = \psi(x + L_x, y) = \psi(x, y + L_y)$ [7]. Instead, we will implement periodicity through magnetic translation operators:

$$T(\mathbf{d}) := e^{-i\mathbf{d}\cdot\mathbf{p}/\hbar} = e^{-i\mathbf{d}\cdot(i\nabla + e\mathbf{A}/\hbar)}, \quad (6.1)$$

which translate a state along a position vector \mathbf{d} . We also define two special cases $T_x = T(\mathbf{d} = (L_x, 0))$ and $T_y = T(\mathbf{d} = (0, L_y))$. We require, as our periodicity condition, that $T_x\psi(x, y) = \psi(x, y)$ and $T_y\psi(x, y) = \psi(x, y)$. The translation operators depend on our gauge choice and in the Landau gauge we have

$$\begin{aligned} T_x\psi(x, y) &= \psi(x + L_x, y) = \psi(x, y), \\ T_y\psi(x, y) &= e^{-ieBL_yx/\hbar}\psi(x, y + L_y) = \psi(x, y). \end{aligned}$$

The last two functions are only equivalent up to a gauge transformation. Additionally, we see that the order of translations matters [7]:

$$T_xT_y = e^{-ieBL_xL_y/\hbar}T_xT_y. \quad (6.2)$$

However, in both cases, we should end up back at the same state. The order in which we translate should not matter. This gives rise to the Dirac quantization condition:

$$\frac{eBL_xL_y}{\hbar} \in 2\pi\mathbb{Z}. \quad (6.3)$$

Now, we can introduce a similar flux as we did in Section 3.1. However, this time the flux is threaded in both the x and y directions. Giving us the resulting gauge potentials,

$$A_x = \frac{\Phi_x}{L_x} \quad \text{and} \quad A_y = \frac{\Phi_y}{L_y} + Bx.$$

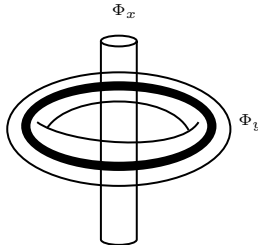


Figure 16: Torus geometry with additional fluxes

This adds an extra term $\Delta H = -\sum_i J_i \Phi_i / L_i$ to the Hamiltonian. Using first order perturbation theory [10], the ground state becomes:

$$|\psi_0\rangle' = |\psi_0\rangle + \sum_{n \neq \psi_0} \frac{\langle n | \Delta H | \psi_0 \rangle}{E_n - E_0} |n\rangle. \quad (6.4)$$

Then, we can calculate the derivative of the state with respect to Φ_i :

$$\left| \frac{\partial \psi_0}{\partial \phi_i} \right\rangle = -\frac{1}{L_i} \sum_{n \neq \psi_0} \frac{\langle n | J_i | \psi_0 \rangle}{E_n - E_0} |n\rangle. \quad (6.5)$$

This looks a lot like the Kubo formula Eq. 4.8, and indeed we can now use that to evaluate the Hall conductivity:

$$\begin{aligned} \sigma_{xy} &= i L_x L_y \hbar \sum_{n=0} \frac{\langle 0 | J_y | n \rangle \langle n | J_x | 0 \rangle - \langle 0 | J_x | n \rangle \langle n | J_y | 0 \rangle}{(E_n - E_0)^2}, \\ &= i \hbar \left[\left\langle \frac{\partial \psi_0}{\partial \phi_y} \middle| \frac{\partial \psi_0}{\partial \phi_x} \right\rangle - \left\langle \frac{\partial \psi_0}{\partial \phi_x} \middle| \frac{\partial \psi_0}{\partial \phi_y} \right\rangle \right]. \end{aligned}$$

Now, we can finally make connections between the Hall conductivity and topology. The fluxes act as parameters in the Hamiltonian. Since these fluxes, also only matter upto mod Φ_0 , we can think of it as periodic and our parameter space would also be a torus \mathbf{T}_Φ^2 . The torus can be parametrized through dimensionless variables $\theta_i = \frac{2\pi\Phi_i}{\Phi_0}$. Thus, since we have a parameter space, we can think about it in terms of the Berry connection and associated field strength. Specifically, we are interested in \mathcal{F}_{xy} :

$$\begin{aligned} \mathcal{F}_{xy} &= \frac{\partial \mathcal{A}_x}{\partial \theta_y} - \frac{\partial \mathcal{A}_y}{\partial \theta_x}, \\ &= -i \frac{\partial}{\partial \theta_y} \langle \psi_0 | \frac{\partial}{\partial \theta_x} | \psi_0 \rangle + i \frac{\partial}{\partial \theta_x} \langle \psi_0 | \frac{\partial}{\partial \theta_y} | \psi_0 \rangle \\ &= i \left[\left\langle \frac{\partial \psi_0}{\partial \theta_y} \middle| \frac{\partial \psi_0}{\partial \theta_x} \right\rangle - \left\langle \frac{\partial \psi_0}{\partial \theta_x} \middle| \frac{\partial \psi_0}{\partial \theta_y} \right\rangle \right], \end{aligned}$$

which looks very similar to our expression for σ_{xy} . In fact, we can write

$$\sigma_{xy} = -\frac{e^2}{\hbar} \mathcal{F}_{xy}. \quad (6.6)$$

More precisely, we have to average over all of the fluxes:

$$\sigma_{xy} = -\frac{e^2}{\hbar} \int_{T_\Phi^2} \frac{d^2 \theta}{(2\pi)^2} \mathcal{F}_{xy}. \quad (6.7)$$

Then we can see that, we can write σ_{xy} as

$$\sigma_{xy} = -\frac{e^2}{2\pi\hbar} C, \quad (6.8)$$

where C is called the first Chern number and

$$C = \frac{1}{2\pi} \int_{T_{\Phi}^2} d^2\theta \mathcal{F}_{xy}. \quad (6.9)$$

Now all that is left to do is to argue that the number C has to be an integer. This can be proved using a similar argument to the Dirac quantization condition or it can be proved more rigorously through an analogue of the **Gauss-Bonnet theorem** in differential geometry [9], which relates the integral of the curvature of a surface, with a global topological invariant called the **genus**. In technical terms, as Ref. [14] shows, the integral of a curvature two-form on the $U(1)$ bundle on a torus will be a integer multiple of 2π , and hence C will be an integer. Thus the quantization of Hall conductance is a topological phenomenon.

7 Conclusion

Overall, in this report, we have highlighted how we can theoretically predict the emergence of the quantized Hall effect. To do this, we explored many tools including Berry's phase, topology, linear response and disorder. We used these tools to explain both the existence of the quantization, as well as why it is robust and remains over a finite range of B values. From here, we could further build on and include interactions in our theory so that we can make predictions about the fractional quantum Hall effect, or we could explore further in the direction of topological insulators.

References

- [1] K. v. Klitzing, G. Dorda, and M. Pepper. New method for high-accuracy determination of the fine-structure constant based on quantized hall resistance. *Phys. Rev. Lett.*, 45:494–497, Aug 1980.
- [2] Beat Jeckelmann and Blaise Jeanneret. The quantum hall effect as an electrical resistance standard. *Reports on Progress in Physics*, 64:1603–1655, 2001.
- [3] R. B. Laughlin. Quantized hall conductivity in two dimensions. *Phys. Rev. B*, 23:5632–5633, May 1981.
- [4] DJ Thouless and M Kohmoto. M. p, nightingale and m. den nijs. *Phys. Rev. Lett*, 49(6):405408, 1982.
- [5] D. C. Tsui, H. L. Stormer, and A. C. Gossard. Two-dimensional magnetotransport in the extreme quantum limit. *Phys. Rev. Lett.*, 48:1559–1562, May 1982.
- [6] Z. Jiang, Y. Zhang, Y.-W. Tan, H.L. Stormer, and P. Kim. Quantum hall effect in graphene. *Solid State Communications*, 143(1):14–19, 2007. Exploring graphene.
- [7] David Tong. Lectures on the quantum hall effect. <https://www.damtp.cam.ac.uk/user/tong/qhe.html>, 2016.

- [8] J. Townsend. *A Modern Approach to Quantum Mechanics*. University Science Books, 2012.
- [9] S.M. Girvin and K. Yang. *Modern Condensed Matter Physics*. Cambridge University Press, 2019.
- [10] J.J. Sakurai and J. Napolitano. *Modern Quantum Mechanics*. Cambridge University Press, 2017.
- [11] M. Nakahara. *Geometry, Topology and Physics, Second Edition*. Graduate student series in physics. Taylor & Francis, 2003.
- [12] C.J. Isham. *Modern Differential Geometry For Physicists (2nd Edition)*. World Scientific Lecture Notes In Physics. World Scientific Publishing Company, 1999.
- [13] S.H. Simon. *The Oxford Solid State Basics*. OUP Oxford, 2013.
- [14] D. Chruscinski and A. Jamiolkowski. *Geometric Phases in Classical and Quantum Mechanics*. Progress in Mathematical Physics. Birkhäuser Boston, 2004.